Mineralogical Magazine, October 2017, Vol. 81(5), pp. 1105–1124

Centennialite, $CaCu_3(OH)_6Cl_2.nH_2O$, $n \approx 0.7$, a new kapellasite-like species, and a reassessment of calumetite

WILSON A. CRICHTON* AND HARALD MÜLLER

ESRF - The European Synchrotron, 71 Avenue des Martyrs, Grenoble 38000, France

[*Received 8 March 2015; Accepted 04 October 2016; Associate Editor: Michael Rumsey*]

ABSTRACT

The new mineral centennialite (IMA 2013-110), $CaCu_3(OH)_6Cl_2{\cdot}nH_2O$, was identified from three cotype specimens originating from the Centennial Mine, Houghton County, Michigan, USA, where it occurs as a secondary product, after acid water action upon supergene Cu mineralization in association with, and essentially indivisible from, other copper-containing minerals such as calumetite and atacamite family minerals. It forms as pale to azure blue encrustations, often taking a botryoidal form. Centennialite is trigonal, $P\bar{3}m1$, $a = 6.6606(9)$ Å, $c = 5.8004(8)$ Å, $V = 222.85(6)$ Å^3, $Z = 1$. The strongest powder X-ray diffraction lines are d_{obs}/Å [I%] (*hkl*), 5.799 [100] (001), 2.583 [75] (201), 2.886 [51] (111), 1.665 [20] (220), 1.605 [17] (023), 1.600 [15] (221), 1.444 [11] (222). The X-ray refined structure forms a kagome net of planar coordinated CuO_4 units with Jahn-Teller coordinated Cl apices to form octahedra that edge-share to in-plane adjacent and flattened CaO_6 octahedra, which are centred about the lattice origin. All oxygen sites are protonated and shared between one Ca-octahedron and one CuO_4 planar unit. Three protonated sites are linked, by hydrogen-bonding to Cl sites, which sit on the triad axis. Each lattice has one Cl above and one below the Ca-Cu polyhedral plane. Consequently, the layers are stacked, along ⟨001⟩, with two Cl sites between layers. In addition to this kapellasite-like topology, an extra *c*/2 site is identified as being variably water-hosting and extends the coordination of the Ca-site to 8-fold, akin to the body-diagonal Pb-Cu sheet in murdochite. Centennialite conforms to the description of the 'Unidentified Cu-Ca-Cl Mineral' noted in Heinrich's *Mineralogy of Michigan* and is almost certainly identical to the supposed hexagonal basic calcium-copper hydroxychloride monohydrate of Erdös *et al.* (1981). We comment upon relationships between calumetite and centennialite and propose a substructure model for a synthetic calumetite-like phase that is related directly to centennialite.

KEYWORDS: calumetite, centennialite, kapellasite, Centennial mine, Houghton County, Michigan.

Introduction

INITIALLY, this study was an attempt to identify the structure of calumetite, $Cu(OH,Cl)_2{\cdot}2H_2O$, first described by Williams (1963) in his work on the minerals occurring in the Centennial mine, Houghton County, Michigan, USA, which included anthonyite, $Cu(OH,Cl)_2{\cdot}3H_2O$, and 'several others'. Both calumetite and anthonyite are not fully described, yet calumetite has since been identified from multiple localities (Brandes and Robinson, 2002; Heinrich and Robinson, 2004; Kumar *et al.*, 2011) and is a possible medieval pigment, of lime-blue colour (Krekel and Polborn, 2003).

Given that the structure was unknown, with a relatively simple proposed chemistry and was readily indexable by its X-ray pattern, 'calumetite' specimens were purchased by the authors (Mikon GmbH). Through inspection of powder X-ray diffraction patterns of samples from these minute specimens, it became apparent that the samples were not calumetite, but were an intimate admixture of minor paratacamite and a material most similar to JCPDS 32-1258†, a hexagonal, basic calcium-

*E-mail: crichton@esrf.fr
https://doi.org/10.1180/minmag.2016.080.157

†Powder XRD file number at the International Centre for Diffraction Data, http://www.icdd.com/

copper hydroxychloride monohydrate, $Cu_3(OH)_6CaCl_2{\cdot}H_2O$, $a = 6.66$ Å, $c = 5.81$ Å, prepared by Erdös *et al.* (1981). Erdös *et al.* (1981) also report that their compound is one of a series of basic hydroxychlorides reported by Feitknecht (1949) and Oswald and Feitknecht (1964), most recently cited through their relation to the new descriptions of kapellasite ($Cu_3Zn(OH)_6Cl_2$) (Krause *et al*., 2006), herbertsmithite (Braithwaite *et al.*, 2004) and haydeeite ($Cu_3Mg(OH)_6Cl_2$) (Schlüter and Malcherek, 2007). Later studies have further developed the crystallization of that same compound, on an industrial scale (Lubej *et al.*, 2004), where it appears (as do other related basic copper salts) as active ingredients of a range of contact fungicides/herbicides akin to Bordeaux mixture. We became more intrigued because Erdös *et al.* (1981) also reported a more hydrated $Cu_4CaCl_2(OH)_8{\cdot}3.5H_2O$ compound (JCPDS 32-1257) that was indexed as primitive tetragonal (a = 9.44, $c = 15.077$ Å) and commented upon as being calumetite-like. When heated to 165°C, this compound is also reported to form $Cu_3(OH)_6CaCl_2{\cdot}H_2O$, apparently the same phase that dominated our natural specimens. None of the structures of these chemistries were elucidated. In the past decade interest in the basic copper hydroxides has increased enormously; several new members as minerals and many more as synthetic compounds with the general atacamite group formula $M^{2+}Cu_3(OH)_6Cl_2$, M^{2+} = Zn, Cu, Ni, Co, Mg, Mn, Cd are already described as atacamite, kapellasite, or otherwise related forms such as gillardite (Braithwaite *et al.*, 2004; Clissold *et al.*, 2007; Fleet, 1975; Kampf *et al.*, 2013*a*; Kampf *et al.*, 2013*b*, Krause *et al.*, 2006; Malcherek and Schlüter, 2007; Malcherek *et al.*, 2014; Nishio-Hamane *et al.*, 2014; Welch *et al*., 2014). These may be highly site-ordered or essentially disordered over the cation sites, particularly in paratacamite structures, with Zn-, Mg- and Ni-dominant intermixing chemistries known. Outside of the mineralogy community this interest is partly due to a singular aspect that their structures share that offers the potential of investigating the properties of geometrically frustrated systems (Chu *et al.*, 2010; Colman *et al.*, 2011; Fak *et al.*, 2012; Jansen *et al.*, 2008; Kermarrec *et al.*, 2014; Li *et al.*, 2013; Li and Zhang, 2013; McQueen *et al.*, 2011; Nilsen *et al.*, 2013). These occur in several geometric situations; for instance, when magnetic ions are arranged in a trihexagonal or honeycomb Ising net (Wannier, 1950). The term 'kagome' was later applied by Husimi (Syozi, 1951) and solutions for which were determined for its specific heat function and lack of magnetic transition. An ideal system for physical study might be arranged in a manner such that the kagome net is planar and where there is sufficient inter-layer separation that one layer does not bias the next layer's magnetic response. Therefore, ideally planar 2D structures are favoured over their three-dimensional counterparts (kapellasite- over herbertsmithite- over murdochite-like topologies, say). In designing such a system, we might then require the largest difference between non-magnetic M^{2+} and Cu cations that will still afford crystallization in this structure type, in order to give the maximum interlayer gap and minimize possible cation site mixing. The compound used by Erdös *et al.* (1981) was Ca-containing and Ca has an ionic radius significantly larger (six-coordinated $Ca^{2+} = 1.00$ Å) than other atacamite, or kapellasite M^{2+} cations (e.g. Mg = 0.72 Å, Zn = 0.75 Å, $Mn^{2+} = 0.83$ Å (high spin); cf. $Cu^{2+} = 0.73$ Å). Due to this potential for further magnetic studies and the potential for slightly different Ca-Cu hydroxychloride hydrates so far mentioned, we also conducted extensive measurements on synthetic compounds; however, here we prioritize this description to those data provided to the Commission on New Minerals, Nomenclature and Classification, and as far as possible, only supported by the three cotypes.

The mineral and name have been approved by the IMA-CMNMC, reference number IMA 2013-110, and is named for the type location, the Centennial mine, Calumet, Houghton County, Michigan, USA, which is part of the Lake Superior native copper district that extends to include Ontonagon, Houghton and Keweenaw Counties of the Northern Peninsula region of Michigan. The three cotypes originate from this location, though at what depth is unclear from cotype 1. The Centennial mine is also the type locality for anthonyite and calumetite. For a complete description of the regional and local mineralogy and setting, the reader is referred to Heinrich's *Mineralogy of Michigan* (Heinrich and Robinson, 2004) and references therein.

Type material

We have elected to use three cotypes as our initial material for centennialite was originally supplied as 'calumetite' and, conversely, initial synthesis trials of the centennialite compound produced a material with a diffraction pattern resembling calumetite. Thus it was our intention to provide evidence that

centennialite can be found with genuine type-specimen calumetite and other pedigreed material donated by Williams. We were kindly given access to specimen 8789 from the Mineral Museum of the University of Arizona, following Williams' note of submission, and specimen 14073 of the Musée de Minéralogie de Paris, as it is listed by the IMA as a type specimen of calumetite. These specimens are now also cotypes of centennialite, in addition to our original cotype 1 material which has been split between the two Institutions as detailed below.

Cotype 1 is the original specimen from which we identified centennialite. It was sold as 'Calumetite: Centennial Mine, Calumet, Houghton Co., Michigan, USA.' Three pieces in gelatine capsules remain with two labels (of an original supply of five: one part has been exhausted, one is an empty capsule and one lacked any material relevant to this study). The contents of the capsules are single agglomerations up to 0.5 mm of detached botryoidal crusts of greenish blue colour and, following X-ray inspection, mixed mineralogy (Fig. 1*a*). The Musée de Minéralogie, Paris and the Mineral Museum of the University of Arizona, have retained part of this sample; with catalogue numbers 83080 and 19588, respectively.

Cotype 2 (Fig. 1*b*) is specified as University of Arizona specimen 8789; 'Calumetite', from 'Centennial Mine, (4.800' level) Mich.' from Sidney A. Williams and was received into the University of Arizona Mineral Museum collection on 01/01/1964 [1st January 1964]. It consists of a single specimen, 50 mm × 25 mm × 20 mm as encrustations in and on wall-rock; with a painted label.

Cotype 3 (Fig. 1*c*) is specified as 'Calumetite' from 'Centennial mine, Calumet, Houghton Co., Michigan, USA (4.800' level), exchange with S.H. [*sic*] Williams, 1963' in the Musée de Minéralogie, Paris, collection number 14073. It consists of several mm-sized irregular encrusted pieces plus a detached grain box-mounted and labelled.

Upon inspection, it transpired that our selection of multiple cotypes was essential, as none individually offered unique identification of characteristic peaks of the title compound by exclusion of other contributions, a general observation also quoted elsewhere; e.g. Brandes and Robinson (2002) and *Mineralogy of Michigan* (Heinrich and Robinson, 2004).

Occurrence

Centennialite is described from the Centennial Mine, Calumet, Houghton County, Michigan, USA, (47°15′30″ N, 88°25′43″ W), which is part of the Lake Superior native copper district that extends to include Ontonagon, Houghton and Keweenaw Counties of the Northern Peninsula region of Michigan. It occurs as a secondary product, after acid water action upon supergene Cu mineralization in association with, and essentially indivisible from, other Cu-containing minerals such as calumetite and atacamite family minerals. For a complete description of the regional and local mineralogy and geological setting, the reader is referred to *Mineralogy of Michigan* (Heinrich and Robinson, 2004) and references therein. The description, association and proposed chemistry of centennialite is identical to that of the 'Unidentified Cu-Ca-Cl Mineral' of the *Mineralogy of Michigan* (Heinrich and Robinson, 2004), which uses a proposed chemistry $Cu_3(OH)_6CaCl_2 \cdot H_2O$? and has been identified at various mines in the district; e.g. Ahmeek (see figs 50 and 144 of *Mineralogy of Michigan;* Heinrich and Robinson, 2004), Quincy, White Pine, Mohawk and Centennial mines, where "*it often occurs with calumetite, which it greatly resembles*." It is proposed, on the basis of X-ray and infrared data (unpublished work of B. C. Cornilsen, cited in *Mineralogy of Michigan*) that this unknown mineral corresponds to the compound of Erdös *et al.* (1981); however, "*…that it is only found in small amounts, intimately mixed with other phases* [therefore] *making it nearly impossible to characterize.*" Further unpublished work since made available to these authors has also highlighted the occurrence of centennialite (in association with calumetite) from those mines listed above and the Franklin Jr. mine (Brandes and Robinson, 2002). Diffraction data and descriptions of the habits from that material (A. W. Seaman Mineral Museum specimens WAS-254, Quincy and WPM-7, White Pines) tested therein are in concordance with these data here; that is, "*calumetite and calcium copper chloride minerals can form as a mixture on the same specimen*." Other specimens, e.g. FS-101, are noted as occurring with both pale and intense dark blue botryoidal masses showing energy dispersive spectroscopy evidence of Cu-Ca-Cl content (Brandes and Robinson, 2002). We emphasize the implication that both field and laboratory investigations on natural samples, where a wider range of locations have been surveyed than here, and synthetic compounds clearly identify a close association between various Ca-Cu hydroxy-chloride hydrates and calumetite (or calumetite-like phases). There is considerable evidence that

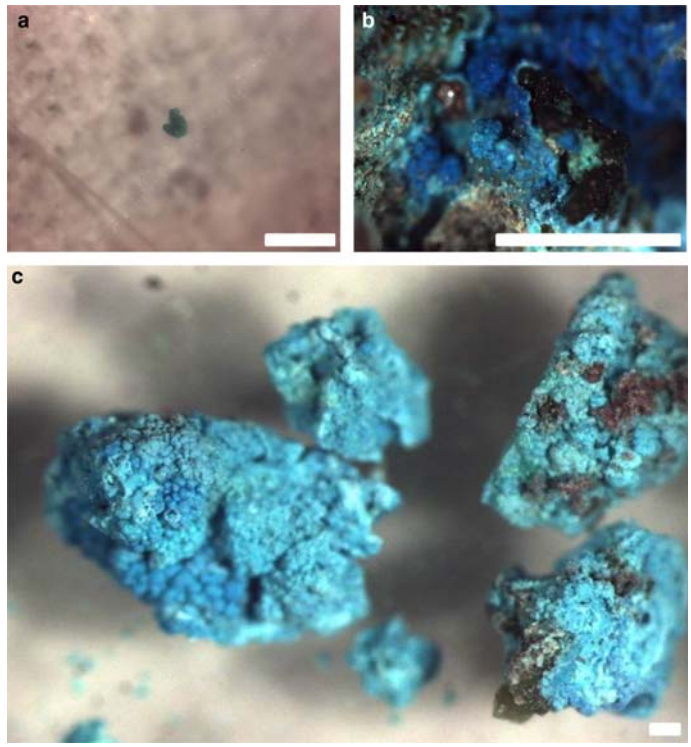

FIG. 1. Photographs of the specimens used in this study, all from the Centennial mine; (*a*) pale greenish blue aggregate of botryoidal crust ~250 μm across, in and through the gelatine capsule – part of cotype 1; (*b*) part of cotype 2 and University of Arizona Mineral Museum specimen 8789 showing a surface coating on copper mineralization, with chalky pale-blue encrustation; (*c*) part of cotype 3 and Musée de Minéralogie, Paris, specimen 14073, showing pale and powder blue regions of centennialite-bearing calumetite. Paler blue regions tend to be richer in centennialite (by X-ray, in transmission). The scale bar is ~0.5 mm in each photograph.

mineralogies corresponding to the hexagonal monohydrate identified by Erdös *et al*. (1981) have been identified elsewhere in field specimens and that these correspond to this description of centennialite.

Optical properties

The material was unsuitable for any type of optical analysis barring simple macroscopic descriptions.

Chemistry

Given the size and the heterogeneity of the natural specimens, analyses of a qualitative and comparative nature were performed to demonstrate presence of Ca in all cotypes. Analysis was performed on a LEO 1530 EM with an Si/Li Oxford INCA system (ESRF). To minimize in-beam degradation of the sample, which resulted in significantly low totals, back-scattering (EDX) area scans were used over a 90 second period. These nonetheless identify an ~1:3:2 atomic ratio in Ca:Cu:Cl composition (Table 1) across all three cotypes.

As more accurate information pertaining specifically to centennialite was not possible on the natural samples, analyses were also performed on synthetic material. To ensure the same phase was analysed, the X-ray pattern of the synthetic compound was confirmed as being indistinguishable from both centennialite and Erdös *et al.*'s hexagonal monohydrate. A combination of combustion analysis, ion chromatography, inductively coupled plasma mass spectrometry and inductively coupled plasma atomic emission spectroscopy, analyses conducted by Mikroanalytisches Labor Pascher, Remagen, Germany, resulted in

TABLE 1. Results of chemical analyses (at.%) of the three cotype specimens conducted by secondary emission in an LEO 1530 electron microscope equipped with a Si/Li Oxford INCA system. Totals are low due to significant beam degradation and area scans were performed to minimize this effect. Note the resemblance of all three cotypes (which are multiphase) to each other and the near 1:3:2 atomic ratio between Ca:Cu:Cl in each. Silver, Zn, Fe and Mg were all sought for but not detected.

Sample Constituent	Area scan	Cotype 1	8789 (ex-Williams) Cotype 2	14073 (ex-Williams) Cotype 3
Al	1	n.t.	n.t.	n.t.
	2	n.t.	n.t.	0.4
	3	0.5	n.m.	n.t.
Si	1	n.t.	n.t.	n.t.
	2	n.t.	n.t.	0.3
	3	n.t.	n.m.	n.t.
Ca	1	10.4	9.9	3.4
	2	10.6	10.2	8.9
	3	9.8	n.m.	8.1
Cu	1	29.0	29.2	36.6
	2	28.8	29.1	30.6
	3	28.9	n.m.	30.4
Cl	1	21.3	21.9	19.9
	2	21.2	21.6	19.1
	3	21.2	n.m.	23.0
O	1	39.4	39.1	40.0
	2	39.4	39.2	40.7
	3	39.5	n.m.	38.5

n.t. = no trace, n.m. = not measured.

composition of Ca 10.1 wt.%, Cu 44.3 wt.%, Cl 16.9 wt.%, O 24.2 wt.%, H 1.91 wt.%, with a total yield of 97.41 wt.%, of which the oxygen analysis is determined as being least reliable. This gives an empirical formula of $Ca_{1.05}Cu_{2.92}(OH)_{5.94}Cl_2 \cdot H_{1.98}O$ (normalized to 2 Cl, with OH and H_2O partitioned according to H content and charge-balancing). Using the inferred water content obtained here, and the structural studies of cotype 1 and cotype 3, the formula for centennialite is $CaCu_3(OH)_6Cl_2.nH_2O$, where $n \approx 0.7$.

X-ray crystallography

Powder diffraction data from a 0.25 mm irregular mass of cotype 1 were collected on a mar555 flat-panel detector in transmission mode at beamline ID09A, at a wavelength of 0.4144 Å and distance of ~310 mm with a Laue monochromated and focused beam size of ~10 μm^2. The friable sample was mounted on adhesive tape and ω was oscillated by −12° to 12° during exposure (3 seconds) to improve intensity averaging. The sample-detector-beam geometry and wavelength was calibrated with a Si standard, using *Fit2D*, (Hammersley *et al.*, 1995), and was subsequently azimuthally integrated to result in a regular 2θ-intensity diffraction pattern (Hammersley *et al.*, 1996). This method was also used for cotypes 2 and 3, while data presented for synthetic samples were collected at beamline ID06, with 0.5 mm capillary samples, in transmission at a monochromatic wavelength of 0.3757 Å, on a mar345 image plate detector. In this case the detector geometry and sample-detector distance was fixed using SRM660a and reduced using *Fit2D*. One additional dataset, of synthetic sample number CaCuOx_60, shown here for comparison only, was collected on a Rigaku Miniflex-II, in flat-plate reflection geometry in θ–2θ mode with Cu$K\alpha$ radiation that was analysed downstream with a graphite (002) monochromator.

Comparisons of the cotypes

Cotype 1, being our original material, was considered the primary specimen and all descriptive structural work uses data collected on this sample. Automated search-match readily assigns all peaks to a mixture of card JCPDS 35-1258 (Erdös *et al.*, 1981 data) (i.e. $Cu_3(OH)_6CaCl_2{\cdot}H_2O$, $a = 6.66$, $c = 5.81$ Å) and minor paratacamite. As no structure is associated with Erdös *et al.*'s phase, we proceeded to index all reflections not assigned to possible paratacamite. Peaks were selected by their 2nd-derivative, without smoothing, on background-subtracted ($y_{min} = 0$) data. From the first 20 unidentified lines, *TAUP* (Taupin, 1973) obtains the hexagonal lattice $a = 6.6589$, $c = 5.8038$ Å, M(20) = 18.36, with a considerable number of primitive and centred orthorhombic and tetragonal lattices, due to an eventual $c/a \approx \sqrt{3}/2$, which allows for notional higher metric symmetry based on an *F*-centred cubic lattice of $a \approx 9.44$ Å. *DICVOL91* (Boultif and Louër, 1991) identifies the hexagonal lattice $a = 6.6586(16)$, $c = 5.8038(17)$ Å with M(20) = 45.7 and F(20) = 146.5, by far the highest rating of these possible solutions. Using the extended list of uniquely indexed peak positions, and minimizing on *d* spacing, a symmetry-constrained lattice is obtained with *Unitcell* (Holland and Redfern, 1997) and results in $a = 6.6606(9)$, $c = 5.8004(4)$ Å, $V = 222.85(6)$ Å^3, identical to that reported by Erdös *et al.* (1981), Table 2. The powder diffraction data were Le Bail-fitted (Le Bail *et al.*, 1988) using *Jana2006* (Petříček *et al.*, 2014) and no systematic extinctions were observed relative to a lattice-restrained *P*1 fit. Using the correspondence with other kapellasite-like structures the symmetry of $P\bar{3}m1$ was deemed appropriate, the structure was filled using a kapellasite basis from Krause *et al.* (2006) and refined (Table 3, Fig. 2), with the inclusion of the substructure model for $Cu_3(OH)_2Cl$ as paratacamite of Fleet (1975). The Le Bail fit of both phases returns a profile GoF = 1.30, *R*p = 2.90%, *wR*p = 4.68%; $a = 6.66421(5)$, $c = 5.81092(8)$ Å and $a = 6.84220(15)$ Å and $c = 14.13015(15)$ Å. Rietveld refinement *R* factors were; for centennialite, *R*obs = 5.99%, *wR*obs = 7.38% and paratacamite Robs = 7.73%, wRobs = 8.54%, with profile GoF = 2.19, Rp = 5.14% and *wR*p = 7.88% with lattices of $a = 6.6615(1)$, $c = 5.8022(2)$ Å, for centennialite and $a = 6.8369(7)$, $c = 14.126(3)$ Å for the $R\bar{3}m$ substructure. These refined values for centennialite are, within error, identical to those obtained by symmetry constrained least-squares and those of Erdös *et al.* (1981).

TABLE 2. Powder diffraction data collected for centennialite. Using *Unitcell* (Holland and Redfern, 1997). These data refine to $a = 6.6606(9)$, $c = 5.8004(4)$ Å and $V = 222.85(5)$ Å^3, using a hexagonal lattice, with no zero correction.

I_{rel}	d_{meas}	d_{calc}	*h*	*k*	*l*
100	**5.799**	**5.800**	**0**	**0**	**1**
1	4.093	4.090	0	1	1
2	3.332	3.330	1	1	0
51	**2.886**	**2.888**	**1**	**1**	**1**
75	**2.583**	**2.582**	**2**	**0**	**1**
<1	2.187	2.187	1	1	2
32	**2.045**	**2.045**	**2**	**0**	**2**
2	1.934	1.933	0	0	3
4	1.834	1.833	0	1	3
5	1.823	1.825	3	0	1
2	1.743	1.743	2	1	2
20	**1.665**	**1.665**	**2**	**2**	**0**
17	**1.605**	**1.606**	**0**	**2**	**3**
15	**1.600**	**1.601**	**2**	**2**	**1**
11	**1.444**	**1.444**	**2**	**2**	**2**
8	1.399	1.399	0	4	1
<1	1.365	1.363	0	3	3
<1	1.330	1.330	1	1	4
<1	1.323	1.323	3	2	0
7	1.296	1.296	0	2	4
6	1.291	1.291	0	4	2
2	1.262	1.262	2	2	3
1	1.232	1.230	4	1	1
<1	1.208	1.207	1	2	4
<1	1.204	1.204	2	3	2
2	1.156	1.156	4	0	3
<1	1.139	1.137	0	1	5
2	1.090	1.090	4	2	0
2	1.077	1.076	0	2	5
4	1.071	1.071	4	2	1
4	1.022	1.023	4	0	4
4	1.020	1.020	4	2	2
1	0.961	0.961	6	0	0
2	0.949	0.950	4	2	3
1	0.912	0.913	6	0	2
<1	0.904	0.904	4	0	5
1	0.871	0.871	4	2	4
<1	0.861	0.861	6	0	3
<1	0.832	0.833	4	4	0
<1	0.824	0.824	5	3	0

The strongest diffraction peaks are shown in bold.

Cotype 2 displays a wide variety of crystallizing mineralogies (Fig. 3). We identify clearly through search match and Le Bail fit (Le Bail *et al.*, 1988), using *Jana2006* (Petříček *et al.*, 2014), these as centennialite: $a = 6.64450(10)$, $c = 5.8006(2)$ Å;

TABLE 3. The structure of centennialite obtained by Rietveld refinement (see Fig. 2), with additional H location by repulsion methods.

Crystal data	
Formula	$CaCu_3(OH)_6Cl_2 \cdot 0.79(3)H_2O$
Formula weight	414.54
Crystal system	trigonal
Space group	$P\bar{3}m1$
Unit-cell dimensions	a = 6.6615(1) Å
	c = 5.8023(2) Å
Cell volume	222.98(2) $Å^3$
Density, calculated	3.100 g cm^{-3}
Pearson code	*hP*19
Wyckoff sequence	i^2edba

*R*obs = 5.99% *wR*obs = 7.38%, refined with paratacamite, to Goof = 2.19 *R*p = 5.14%, *wR*p = 7.88%.

Atom coordinates

Atom	Wyck.	Occ.	*x*/*a*	*y*/*b*	*z*/*c*	*U*, $Å^2$
Cu1	3*e*		½	0	0	0.0194(4)
Ca1	1*a*		0	0	0	0.037(2)
O1	6*i*		0.1903(7)	0.8097	–0.1434(9)	0.0255(17)
Cl1	2*d*		1/3	2/3	0.3791(9)	0.0258(14)
H†	6*i*		0.1909(15)	0.8091(8)	–0.3012(6)	0.038
Ow	1*b*	0.79(3)	0	0	½	0.066(8)
Distances						
Cu1–O1	4×	1.985(4) Å	Ca1–O1	6× 2.348(5) Å	Ca1–Ow	2× *c*/2 Å
Cu1–Cl1	2×	2.922(4) Å	O1–H1	1× 0.916(5) Å		
Angles						
O1–Cu–Cl		92.78(13)°				
O1–H···Cl1		138.9(3)°				

†Unrefined and located by repulsion, see text; errors on H by standard deviation over 10 runs in *P*1.

calumetite (Erdös *et al.*'s proposed lattice in $P4_2$); *a* = 9.39363(11), *c* = 15.081(3) Å and clino-atacamite, *a* = 11.8487(6), *b* = 6.8191(4), *c* = 6.1690(3) Å, β = 130.777(4)°, space group $P2_1/a$. All samples taken from cotype 2 display these components in varying degrees. Cotype 3, the type-specimen of calumetite, showed a similar range of minerals (Fig. 4), with the addition of what is probably a small amount of (pseudo)boleite, identified on the basis of its large *d* spacings (and the association with atacamite-like minerals is described elsewhere, e.g. La Compania mine, Sierra Gorda, *etc*.). The variation was more pronounced in this specimen so that in one scan an almost ideal centennialite pattern was obtained (Fig. 5), which was subsequently fitted to GoF = 0.75, *R*p = 1.95%, *wR*p = 3.81%; *a* = 6.64066 (8), *c* = 5.79836(22) Å in space group $P\bar{3}m1$.

Crystal structure

The crystal structure of centennialite, Fig. 6, consists of a two-dimensional triangular network of edge-sharing CaO_6 octahedra, located at the vertices of the hexagonal lattice. These alternate with edge-sharing planar CuO_4 units at *a*/2 such that each CaO_6 octahedron is surrounded by rectangular CuO_4 units, three of which have identical tilt planes with respect to the *aa* plane. All O sites are protonated and bridge Ca and Cu sites. This Ca-Cu-polyhedral layer is separated

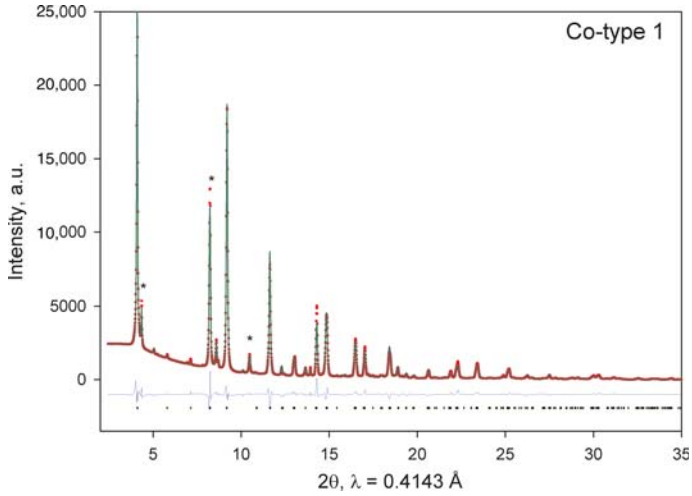

FIG. 2. X-ray diffraction pattern produced by Rietveld refining the centennialite model (shown in Table 3) against X-ray data taken at ID09A, Mar555 detector, λ = 0.4143 Å. It contains centennialite and paratacamite only. The Le Bail fit of both phases returns GoF = 1.30, *Rp* = 2.90%, *wRp* = 4.68%; *a* = 6.66421(5), *c* = 5.81092(8) Å and *a* = 6.84220(15) Å and *c* = 14.13015(15) Å (Fleet (1975) substructure, as $Cu_2(OH)_3Cl$). Rietveld refinement *R* factors were, for centennialite, *R*obs = 5.99%, *wR*obs = 7.38%, and for paratacamite *R*obs = 7.73%, *wR*obs = 8.54%, with profile GoF = 2.19, *R*p = 5.14% and *wR*p = 7.88%. Peak position data in Table 2 and Table 4 are from this dataset.

from the next, at one lattice spacing along *c*, by hydrogen-bonding to Cl sites. One Cl site is located above the layer, and one below, so that there are two Cl positions between each adjacent pair of layers. These extend the coordination to form the long apices of Jahn-Teller distorted $Cu(OH)_4Cl_2$

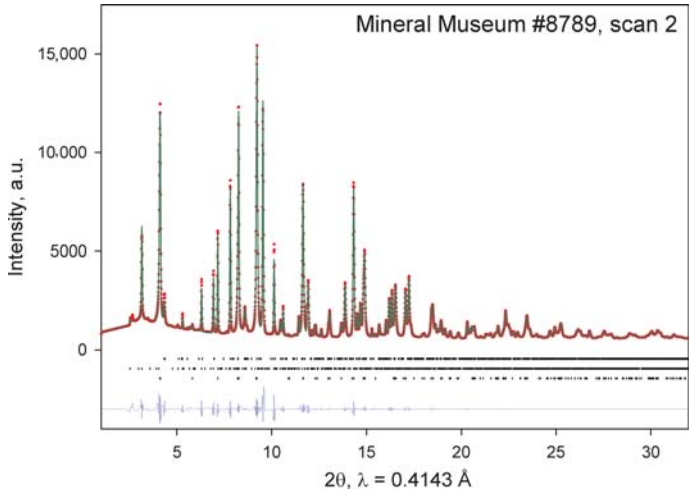

FIG. 3. Le Bail fitted X-ray diffraction pattern of part of specimen 8789 (cotype 2) showing centennialite, calumetite and clinoatacamite. Fitting uses a $P\bar{3}m1$ lattice (for centennialite), a $P4_2$ lattice (simulating Erdös *et al.*'s proposed lattice) and a monoclinic clinoatacamite lattice. GoF = 1.61, *R*p = 2.52%, *wR*p = 4.58%. Tick-marks under the pattern: 'centennialite': *a* = 6.64450(10); *c* = 5.8006(2) Å; calumetite (estimated sublattice); *a* = 9.39363(11), *c* = 15.081(3) Å; clinoatacamite, *a* = 11.8487(6), *b* = 6.8191(4), *c* = 6.1690(3) Å, β = 130.777(4)° (in $P2_1/a$). Observed points are shown in red and the calculated line is green. Data collection is as per Fig. 2.

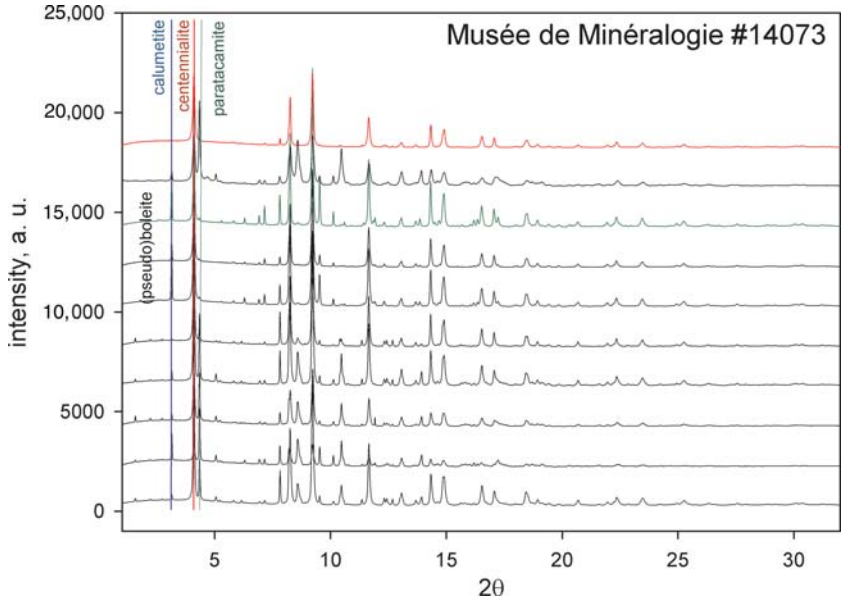

FIG. 4. X-ray survey of parts of Musée de Minéralogie specimen 14073 (type of calumetite and cotype 3 of centennialite) showing the variety of mineral phases in this material. Highlighted in red is the sole, near-clean centennialite obtained in our survey and in green the closest approximation to samples of 8789. Vertical rules indicate the location of the main diffraction peaks of calumetite, centennialite and paratacamite. Large *d* spacings of possible pseudoboleite are indicated. Data collection is as per Fig. 2.

octahedra. We have no significant evidence of site intermixing. Atom–atom distances are highly constrained by bridging and the lattice point symmetry; thus Ca–Ca = *a*, and Cu–Ca and Cu–Cu = *a*/2. Cu–O and Ca–O can vary but there is one unique value per lattice for each, at 4 × 1.985(5) Å

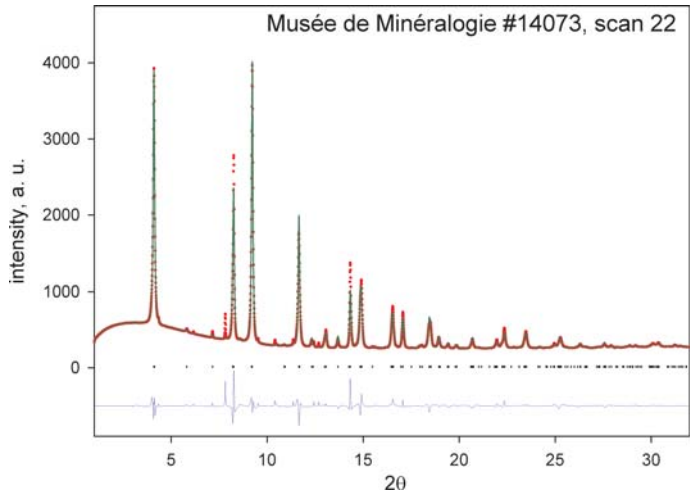

FIG. 5. A profile fit of the near clean centennialite pattern (shown in red, Fig. 4) obtained from cotype 3. ID09A data, fitted with Jana2006 to GoF = 0.75, *R*p = 1.95%, *wR*p = 3.81%; *a* = 6.64066(8), *c* = 5.79836(22) Å in space group $P\bar{3}m1$. Rietveld refinement of the centennialite model proposed here against these data results in a near identical structure with Ow occupancy of 0.70(4).

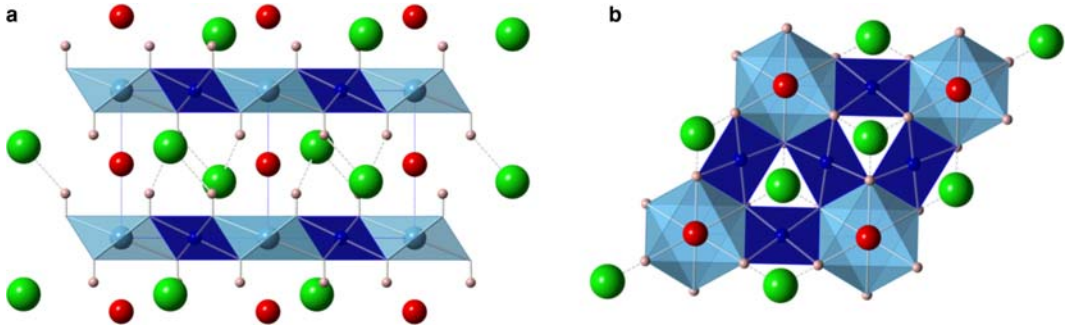

FIG. 6. The refined structure, shown in Table 3, of centennialite. The chloride ions (green) lie on a triad axis about which three identical (dark blue) planar $CuO(H)_4$ units are positioned and edge share *via* bridging oxygens to (sky blue) $CaO(H)_6$ octahedra. The bridging oxygen sites are protonated and form hydrogen bonds to the intralayer chlorides, of which there are two between each layer, per lattice. Additionally, a *c*/2 oxygen (water) is shown in red. The coordination of Ca, extended to these is displayed in Fig. 7, shown along the diagonal diad (*a*) and in the *aa* plane (*b*).

and 6 × 2.348(5) Å. Inspection of the Rietveld-refined lattice (*a* = 6.6615(1), *c* = 5.8023(2) Å) and comparison with other kapellasite-like minerals, indicates that our presumptions with respect to the effect of ion size are not misplaced. The necessity of site symmetry to self-constrain all bonds between Ca and Cu with O(H) at reasonable lengths has the effect of further flattening the octahedra, which show an elongation of 1.1558; cf. 1.0698 (haydeeite; Schlüter and Malcherek, 2007), or 1.0771 (kapellasite; Krause *et al.*, 2006) and larger cell parameters in both directions (including misakiite, where we assume high-spin Mn; Nishio-Hamane *et al.*, 2014). We also note that the extension of *c*/*a* as a function of ionic radius is linear for the three larger ionic radius structures. The Cu–Cl distances are longer in centennialite (2.922(4) Å, at 90 ± 2.78(13)° from off-normal to the Cu–O plane) compared to essentially identical values of 2.765 Å in haydeeite and 2.762 Å in kapellasite. We note the value obtained by neutron diffraction for the synthetic analogue is shorter at 2.689 Å (Colman *et al.*, 2008).

In an attempt to locate the hydrogen positions, we used the charge repulsion routine of *ENDEAVOUR*, where minimum constrained distances of O^{2-}–H^{+}_{min} = 0.90 Å, $H^{+}\cdots Cl^{-}$ = 2.22 Å, $Ca^{2+}\cdots H^{+}$ = 2.86 Å, $Cu^{2+}\cdots H^{+}$ = 2.38 Å, $H^{+}\cdots H^{+}$ = 1.52 Å were used. The average H location after 10 runs within the otherwise fixed and refined structure was identified at the 6*i* position near-perpendicular, 89.3(5)°, to the Ca-Cu-polyhedral layer (with H located at 0.3818(15), 0.1909(8), 0.3012(6), in *P*1, that was further symmetrized). This results in the O–H direction lying subparallel to and pointing towards the triad and tending towards the nearer Cl site. The proposed position does then have a O–H distance of 0.916(5) Å, with H···Cl of 2.478(7) Å the O–H···Cl angle of 138.9(4)° and O···Cl of 3.225(7) Å. As expected, given the lattice, these distances are longer than in haydeeite and kapellasite, and longer also than in leverettite, 2.32(3) Å and 3.079(3) Å and gillardite, at 2.26 Å and 3.071 Å (Kampf *et al.*, 2013*a*; Clissold *et al*., 2007).

The main difference between centennialite- and the kapellasite-type structures is the propensity in the synthetic compounds for excess water, of apparently non-integer and variable amount. This aspect of the structure resolution was problematic as, while clear electron density was present at *c*/2, it is not in other kapellasites. The symmetry of an ordered water molecule is not commensurate with trigonal symmetry at that position. Thermogravimetry did not prove useful due to the presence of absorbed H_2O in starting compounds. There is also no suggestion of superlattice peaks that may indicate an alternate symmetry, due to ordering of the Ow site. Infrared data (synthetic) were not definitive either, as the structure already contains water. We required low-temperature neutron refinement of our own synthetic deuterated compounds, together with the chemistry and thermogravimetric results of Erdös *et al.* (1981) and Lubej *et al.* (2004) and our own H-determining microanalysis on synthetic equivalents to be convinced that the *c*/2 site does indeed contain water, that it is disordered, probably variable to *n* = 1, and is not, for instance, a phantom peak in the Fourier maps. The Ow site extends the most distorted M^{2+} octahedra observed in this family to more regular CaO_8

TABLE 4. Comparison between measured *d* spacings and intensities for centennialite and the centennialite-like compound synthesized by Erdös *et al.* (1981).

Measured (this study)		Calculated (Erdös *et al.*, 1981)	
I_{rel}	d_{meas}	I_{rel}	d_{meas}
100	5.799	100	5.806
		40	5.780
1	4.093	20	4.094
2	3.332	30	3.333
		40	2.906
51	2.886	80	2.892
		40	2.597
75	2.583	90	2.581
<1	2.187		2.187
32	2.045	60	2.049
2	1.934	10	1.938
4	1.834	30	1.836
5	1.823	30	1.825
2	1.743	30	1.745
20	1.665	50	1.666
17	1.605	40	1.609
15	1.600	50	1.600
11	1.444	50	1.445
8	1.399	40	1.400
<1	1.365		1.363
<1	1.330		1.330
<1	1.323		1.323
7	1.296	40	1.298
6	1.291	40	1.293
2	1.262	30	1.264

polyhedra. While this is unknown for kapellasites, a view from the origin to planes adjacent to the body diagonal in murdochite, $PbCu_6O_8$ (Christ and Clark, 1955; Dubler *et al.*, 1983), shows a distribution identical to one layer of centennialite, including dry PbO_8 units (ionic radius of eight-coordinate Pb^{4+} = 0.94 Å), Fig. 7. We have since become aware of further single-crystal analyses of synthetic material that corroborates these findings (with one analysis yielding refined occupancy of Ow = 0.61 (S. Pam, pers. comm.). Therefore, the larger ionic radius of Ca^{2+} compared to other kapellasites contributes significantly to the longer lattice parameters and atom–atom distances. This, we believe, is an important demonstration of centennialite's desirability for further magnetic studies, where interlayer interaction should be minimized, especially in the case of an $n = 0$ sample. Any O–H···Cl mediated interaction cannot be avoided, however. From our experience with a wide range of synthetic chemistries and from an ionic radii-bound mechanical model construction, we believe divalent compounds of similar stoichiometry (i.e. protonated structures) may be already limited to Ca-containing (for those crystallizing as kapellasite-like) and Sr-containing (for calumetite-like) compounds.

Discussion

As noted here and elsewhere, there is regular significant admixture of calumetite with centennialite and other phases, rendering identification problematic. Furthermore, our early synthetic runs, aimed at producing centennialite, produced

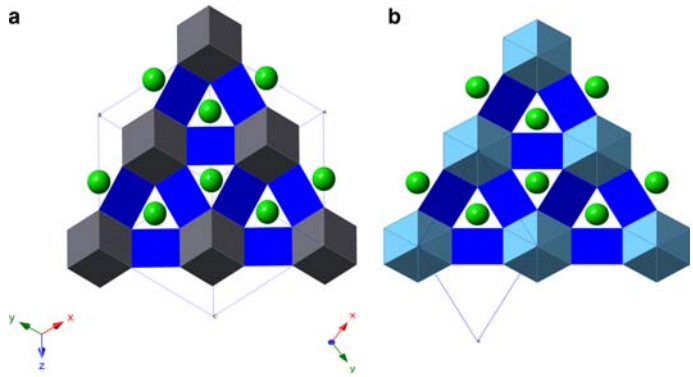

FIG. 7. The schematic representation of the (in-plane) polyhedral construction of murdochite, $PbCu_6O_8$, here shown on its body-diagonal plane (*a*). The manner in which the PbO_8 units link (in this plane) is remarkably similar to that proposed here for centennialite (*b*), shown here with the Ca coordination extended to the Ow site at *c*/2 from the origin (and Ca site).

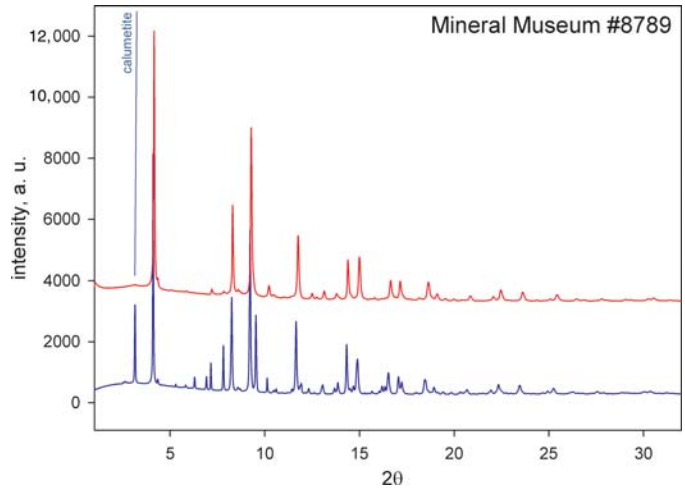

FIG. 8. A sample of specimen 8789, containing both centennialite and calumetite (indicated) was X-rayed before (blue) and after heating for 1 h at 165°C in a normal oven. There is clear loss of those peaks associated with centennialite, but no evidence of a new phase crystallizing, leaving a calumetite-like dominated pattern. This is the 'natural' demonstration of the measurements carried out by Erdös *et al.* (1981) on synthetic material. Diffraction conditions are as per Fig. 2.

instead calumetite-like patterns, or mixtures of the two, clearly indicating their close relationship. Erdös *et al.* (1981) have already demonstrated the similarity of diffraction data for $CaCu_4(OH)_8Cl_2{\cdot}3½H_2O$ and Williams' calumetite, $Cu(OH,Cl)_2{\cdot}2H_2O$ (Williams, 1963). To illuminate this point further, we repeated the Erdös *et al.* heating experiment, where synthetic tetragonal $Cu_4(OH)_8CaCl_2{\cdot}3.5H_2O$ was transformed to hexagonal $Cu_3(OH)_6CaCl_2{\cdot}H_2O$ (of Erdös *et al.*), (now centennialite) on a portion of calumetite from cotype 2. Comparing diffraction patterns before and

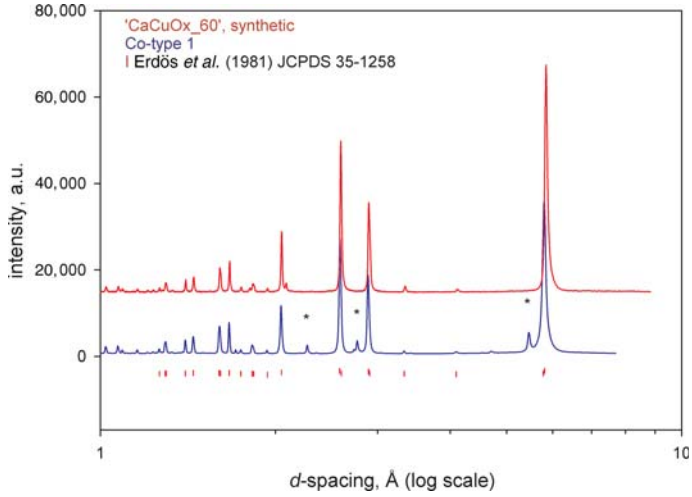

FIG. 9. A comparison (on log scale to de-emphasize the compression of short *d* spacings) of Cotype 1 data, identical to those above (blue) with one of our several synthetic analogues (red; sample 'CuCaOx_60'). We also include data (red ticks) from Erdös *et al.* (1981) on the centennialite-like phase they have produced, following treatment of their calumetite-like compound. The additional peaks (*) are from a minor paratacamite fraction. Note: the original data were collected at different wavelengths, red data (synthetic were collected using Cu$K\alpha$), blue data as for Fig. 2.

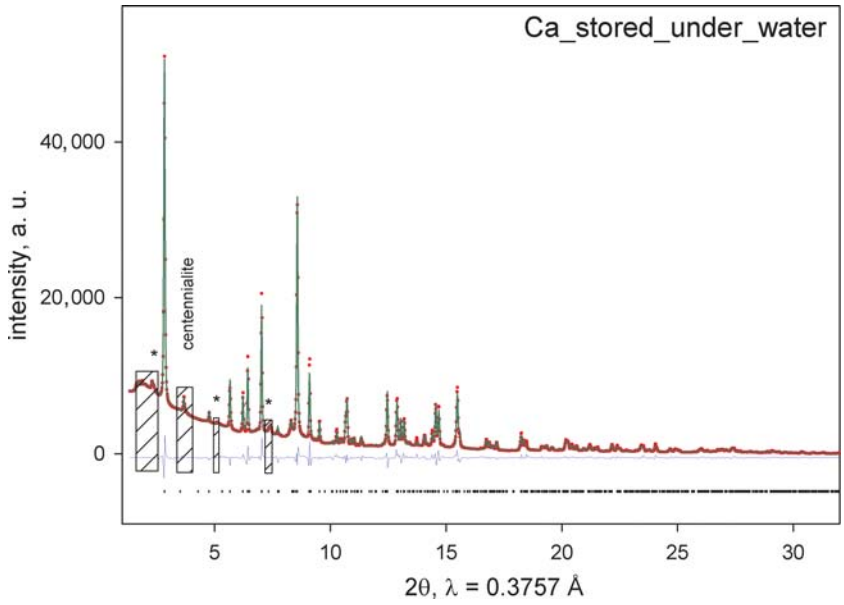

FIG. 10. Rietveld refinement of the *Cmcm* model, Table 6, of synthetic calumetite-like material against data collected on a synthetic sample stored since synthesis under aqueous solution. The excluded regions are those also indicated as unindexed by this over-generalized model in Table 5, apart from that noted 'centennialite'. Data were taken at ID06 at 33 keV in a capillary-mounted sample, in transmission, on a mar345 detector. GoF = 3.49, *R*p = 5.69%, *wR*p = 8.35%, *R*(obs) = 6.63%, *wR*(obs) = 7.80%, *R*(all) = 6.81%, *wR*(all) = 7.83%.

after heating to 165°C, Fig. 8, it is quite clear that the original natural calumetite (with minor paratacamite) sample was converted to one of a near-clean centennialite-like compound, with the addition of no further X-ray lines associated with non-volatile components. Therefore, our natural sample of calumetite, from Williams, is centennialite-like once heated. Erdös *et al.* (1981) can not have been aware of centennialite, but we do confirm that their diffraction pattern and proposed chemistry closely resembles our own targeted synthesis as well as those data taken for cotype 1, Fig. 9 and Table 4. There is a clear relationship between calumetite and centennialite and their proposed synthetic equivalents. Comparing Erdös *et al.*'s and Williams' proposed chemistries (and those here) suggests that Ca might be substitutable with Cu in calumetite, with Williams describing a Cu end-member. We might also expect that more calumetite analogues should be known as many other M^{2+} site chemistries would be more compatible based on closer ionic radii and coordination to Cu than Ca – especially given the number of different M^{2+} atacamite-like chemistries now described. However, this is not the case and suggests rather that calumetite does contain essential Ca – indeed, no analysis we have obtained, suggests otherwise and syntheses directed at a Cu end-member fail.

A model for calumetite

The structure of calumetite has, in spite of its apparently readily indexed reflections, remained unsolved during the 50 years since its description. The primary reason, we suspect, is that it is highly pseudosymmetric. Secondly, there is evidence of stacking disorder from the peak-shape of very weak reflections associated with lattices larger than those based on stronger peaks. Thirdly, there is an evident distinct lack of analogues from synthetic or natural samples and even the singular synthetic example from Erdös *et al.* (1981) has a different reported chemistry and lacks a structure. Lastly, calumetite is rare and no crystals suitable for single-crystal X-ray analysis are known. Using the synthetic calumetite-like compound mentioned previously, that will convert to a centennialite-like analogue upon heating and that has been stored under aqueous liquor since synthesis, we can approach a suitable model for the substructure. It has a highly pseudotetragonal lattice, which can be obtained

TABLE 5. Comparison between the observed data for Erdös *et al.* (1981)'s diffraction data for calumetite-like $CaCu_4(OH)_8Cl_2 \cdot 3.5H_2O$ and data calculated for the refined *Cmcm* two layer model, the $P2_1/c$ superstructure based on this and those data of Williams for calumetite. Erdös *et al.*'s index lattice (*tP*, $a = 9.44$, $c = 15.2$ Å) is related to the *Cmcm lattice* ($a' = b' \approx \sqrt{2}a_{Cmcm} \approx \sqrt{2}c_{Cmcm}$; $c' = b_{Cmcm}$) and to the two layer ordered superstructure by orthogonalization of the lattice. Both our observations and those of Erdös *et al.* require a lattice larger than that proposed by *Cmcm*. The last columns compare the appropriate lines with those of Williams (1963) for calumetite, and are indicated in bold.

Measured		*Cmcm* model		$P2_1/c$ model	Williams calumetite	
*I*rel	*d*meas	*I*rel**	*hk*l**	*hkl**	*I*rel***	*d*meas***
20	9.4			100		
100	**7.54**	**100**	**020**	**020**	**100**	**7.5**
20	6.08	<1	110	$\bar{1}11/111$		
40	4.48	3	111	012		
10	4.196			$\bar{1}02$		
40	**3.777**	**14**	**040**	**040**	**50**	**3.76**
40	**3.428**	**10**	**131**	**032**	**30**	**3.42**
70	**3.32**	**8**	**200**	**202**	**30**	**3.3**
10	3.128			300		
80	**3.037**	**16**	**220**	**222**	**60**	**3.02**
		16	022	$\bar{2}22$		
10	2.917	3	112	$\bar{3}11$		
10	2.768	3	221	321		
10	2.554	6	132	$\bar{1}33$		
90	**2.492**	**34**	**042**	**$\bar{2}$42**	**80**	**2.481**
		41	240	242		
70	**2.348**	**19**	**202**	**004**	**30**	**2.341**
10	2.276			$\bar{1}04/104$		
30	2.242	5	222	420		
40	2.08	3	311	412		
		<1	113	$\bar{2}14$		
10	2.003	3	062	$\bar{2}62$		
		5	260	262		
40	**1.993**	**14**	**242**	**440**	**30**	**1.993**
10	1.958	2	171	072		
20	1.938	1	331	234		
		2	133	$\bar{4}32$		
10	1.886	4	080	080		
10	1.878			015		
10	1.743			$\bar{5}02/502$		
10	1.743	1	172	$\bar{1}72/173$		
40	**1.716**	**16**	**262**	**064**	**30**	**1.709**
60	**1.66**	**9**	**004**	**$\bar{4}$04**	**20**	**1.656**
		7	**400**	**404**		
40	**1.64**	**5**	**082**	**$\bar{2}$82**	**20**	**1.635**
		5	**280**	**282**		
50	1.621	4	024	$\bar{4}24$		
		3	420	424		
30	1.557	2	313	016		
20	1.52	2	044	$\bar{4}44$		
		2	404	444		
40	1.485	3	402	206		
		2	204	561		
30	**1.47**	**18**	**282**	**480**	**20**	**1.465**

(continued)

TABLE 5. (*contd*.)

Measured		*Cmcm* model		$P2_1/c$ model	Williams calumetite	
*I*rel	*d*meas	*I*rel**	*hkl***	*hkl**	*I*rel***	*d*meas***
50	1.457	5	224	$\bar{2}26$		
		7	422	622		
50	**1.381**	**10**	**442**	**246**	**20**	**1.378**
		13	244	$\bar{2}46$		
20	1.373	2	2.10.0	$\bar{2}$.10.2		
		3	0.10.2	2.10.2		
20	1.278	2	264	$\bar{2}66$		
		1	462	662		
20	1.27	2	2.10.2	4.10.0		
20	1.262	<1	135/531	$\bar{4}$36/634		
20	1.258	1	0.12.0	0.12.0		
30	1.247	3	480	484		
		2	084	$\bar{4}$84		
40	1.174	3	0.12.2	$\bar{2}$.12.2		
		2	2.12.0	2.12.2		
20	1.166	3	284	1.10.5		
		2	482	3.12.0		
20	1.16	2	424	028		

*Two-layer $P2_1/c$ model; if orthometric, equivalent to Erdös *et al.* (1981).
**Two-layer *Cmcm* model.
***Calumetite (Williams, 1963).

through autoindexing available powder data, Fig. 10, Table 5. The basic lattice (ignoring asymmetric superlattice peaks) has half the volume of that proposed by Erdös *et al.* (1981),

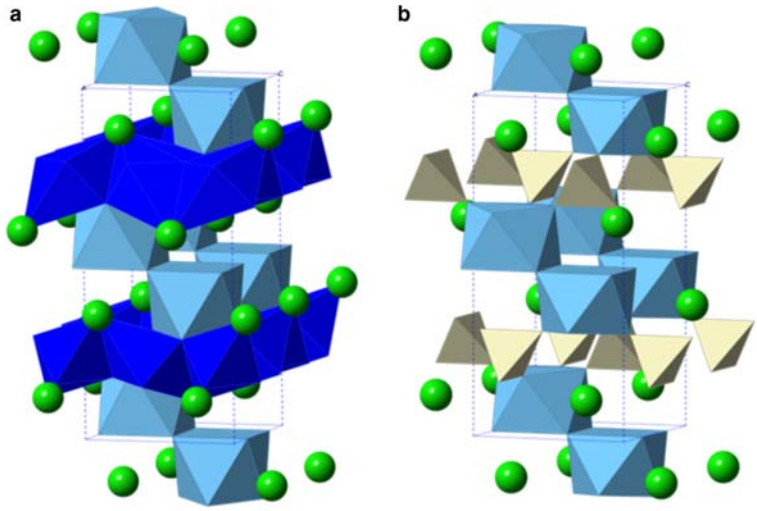

FIG. 11. Polyhedral representations of the proposed two layer substructure model, in *Cmcm*, for centennialite (*a*) compared with that for $CaCl_2(ReO_4)\cdot 2H_2O$ (*b*), of Jarek *et al.* (2007), also *Cmcm*. In both cases the edge-sharing $Ca(OH,H_2O)_8$ polyhedral stacking is evident and between these lie sheets of distorted $Cu(OH,Cl)_6$ octahedra. The Ca sites here are intended as notionally equally half-occupied.

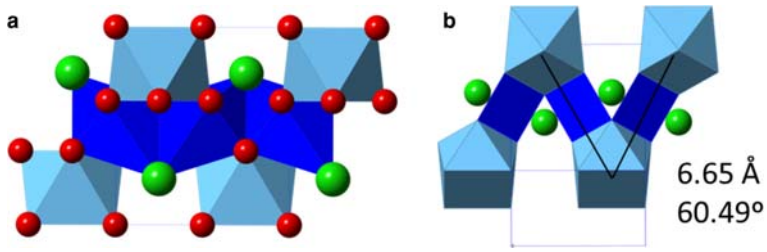

FIG. 12. Polyhedral representation of the proposed *Cmcm* substructure, simplified to a one layer reduction. The mid-plane Cu octahedra form an in-plane sheet with Cl and Ca in the interlayer between them (*a*). The overall orientation differs from that of centennialite, but shares many features (*b*); atom–atom distances are very similar, as are their relative arrangements.

with $a \approx c \approx 6.66$, $b = 15.2$ Å, and will profile refine to a low GoF of −1.5%. *Cmcm* spacegroup symmetry was chosen on the basis of highest symmetry/best fit ratio in a forced orthorhombic lattice. Using this, a solution was obtained rapidly through inspection of Fourier maps and, with atom

TABLE 6. Refined calumetite-like substructure model, in *Cmcm*, with R(obs) = 6.63%, wR(obs) = 7.80%, R(all) = 6.81%, wR(all) = 7.83%.

Crystal data	
Formula sum	Ca2 Cl4 Cu8 O24
Formula	$CaCu_4(OH)_8Cl_2 \cdot 4H_2O$
Z	2
Formula weight	1114.32 (dry)
Crystal system	Orthorhombic
Space group	*Cmcm*
Unit-cell dimensions	$a = 6.696(1)$ Å
	$b = 15.2146(7)$ Å
	$c = 6.703(1)$ Å
Cell volume	682.88(15) Å^3
Density, calculated	2.709 g cm^{-3} (dry)
Pearson code	*oC*40 (dry)
Formula type	NO2P4Q12
Wyckoff sequence	*gfedc2*

Atom coordinates

Atom	Wyck.	Occ.	*x*/*a*	*y*/*b*	*z*/*c*	*U*, Å^2
Ca1	4*c*	0.5	0	0.5887(8)	0.75	0.011(3)
Cu1	8*d*		0.75	0.25	0	0.0122(5)
Cl1	4*c*		0.5	0.37592(6)	0.7500	0.030(2)
O1	8*f*		0	0.3247(13)	0.985(4)	0.026(5)
O2	8*e*		0.724(6)	0	0.5	0.081(6)
O3	8*g*		0.814(2)	0.1888(14)	0.75	0.009(5)

Distances			
Cu1–O2	2× 1.962(10) Å	Ca1–O1	2× 2.21(2) Å
Cu1–O1	2× 2.028(11) Å	Ca1–O2	4× 2.62(2) Å
Cu1–Cl1	2× 3.046(6) Å	Ca1–Ow	2× 2.596(19) Å
Cu1–Ca1	2× 3.410(9) Å		

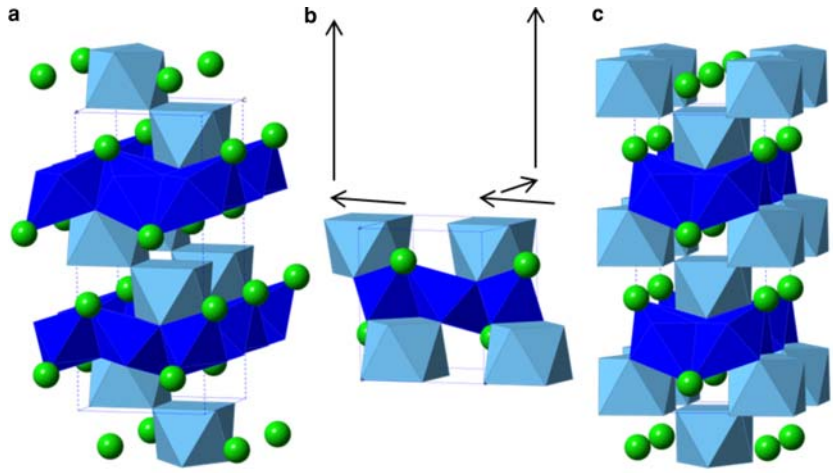

FIG. 13. The *Cmcm* (*a*) model can be produced by stacking the single layer tetragonal layer, also shown in Fig. 11, (*b*), by ½ 0 1, so that the CaO_8 units edge-share; or, by ½ ½ 1 to produce a two-layer, corner-shared, structure that, with orthorhombic distortion, has symmetry *Pmm2* (*c*) and the same lattice size as (*a*). Without this distortion the two layer structure is otherwise absolutely identical to the single layer, as the stacking vector mimics the *n* glide.

reassignment (and a ½ occupied Ca site), reduces to a construction that shares features that we might expect from comparison with the structure of centennialite. These include that the Ca–Cl–Ca–Cl direction is now parallel with the stacking direction (at 60° previously and 15.2 Å ≈ sin(60°) *3$c_{centennialite}$ Å), effectively placing the Cu–Cu polyhedral sheet in-plane, as opposed to the Ca–Cu sheet, Fig. 11*a*. The like-like anion–anion distances define the lattice dimension in an identical manner and the same size as centennialite. The Ca–Ca–Ca angle remains at ≈60° and same-layer Ca sites are 6.8201(4) Å apart, with Cu half way along the same vectors, again as per centennialite, Fig. 11*b*. Indeed, in all aspects bar one *a*|| Ca–Ca direction, where it lacks the intermediate Cu, it is a very closely related topology – though not a subgroup, distortion, or similar construction. The Ca-polyhedra continue to be eight coordinated as per centennialite. As in the comparison between CaO_8 in centennialite and PbO_8 polyhedra in murdochite, this coordination and the edge-sharing linkage between adjacent stacking units is found elsewhere, in the rather similar compound $CaCl(ReO_4)\cdot 2H_2O$, for instance (Jarek *et al.*, 2007; Fig. 12). This *Cmcm* model will fit with *R*obs = 6.64%, *wR*obs = 7.82%, *R*all 6.82% and *wR*all 7.85 with profile *R*p of 5.69% and *wR*p = 8.35% when all structural features are refined (Fig. 10, Table 6). It may then be considered reasonable. However, it does not take into account the few asymmetric peaks that remain unindexed with a lattice this size, which can be seen in Fig. 10 as excluded regions, from the data of Erdös *et al.* (1981); particularly the peak at 9.44 Å, which is not reported by Williams (1963), Table 5.

To address the peak asymmetry, the stacking vector of ½ 0 1 (*Cmcm*), Fig. 13*a*, can be supplemented by corner-sharing the Ca-polyhedra through stacking ½ ½ 1 one unit with respect to the previous. This second model structure, (Fig. 13*c*), produced using Diffax+ (Leoni *et al.*, 2004) reduces to *Pmm2* and remains strongly pseudosymmetric, by lattice distortion only, towards a *c*/2 reduction to the single-layer tetragonal basis with *P*4/*nmm* symmetry (Fig. 13*b*; see the crystallographic information files which have been deposited with the Principal Editor of *Mineralogical Magazine* and are available from http://www.minersoc.org/pages/e_journals/dep_mat_mm.html). It may be no coincidence that this lattice basis will also index all bar the 3.43 Å peak (a *c*-doubled 113, or *Cmcm* 131) of the lower-resolution data of Williams (LSQ $a = 6.620(3)$, $c = 7.515(6)$ Å, *UNITCELL*). A comparison of the calculated intensity distribution is also reasonable. A related lattice (but different diffraction pattern) is found in an *I*-centred, but $\sqrt{2} \times \sqrt{2}$ larger, tetragonal hemihydrate also described by Erdös *et al.* (1981). This phase (JCPDS 35-1528) has composition $CaCu_4(OH)_8Cl_2\cdot 0.5H_2O$ and our model assembly

is, per a *P*4/*nmm* layer repeat, a rather similar $CaCu_4O_{12}Cl_2$. Repartitioning the anions so that assumed O = OH or H_2O gives a composition of $CaCu_4(OH)_8Cl_2{\cdot}4H_2O$, with all interlayer Ow sites fully occupied, is almost identical to Erdös *et al.* (1981)'s proposed calumetite-like compound; with only ½ mol H_2O excess per formula unit. Normalizing to a centennialite-like Cu = 3 (equivalent $Z_{centennialite} = 8/3$, not 3), would result in a composition of $Ca_{0.75}\square_{0.25}Cu_3(OH)_6Cl_2{\cdot}3H_2O$. In a manner analogous to the rhenate example above (Fig. 12), the in-layer O sites are assigned to (OH) and those creating the eight-fold coordination to Ca, water. This may be the reason for why calumetite-like analogues, or minerals, have not been identified from the remainder of the atacamite family, in much the same way that centennialite can be differentiated from the kapellasites. Regardless of available data suggesting such a large lattice, here and in Erdös *et al.* (1981), we have not encountered data that will support any more detailed refinement without recourse to excessive use of constraints, or any indexation that is markedly non-pseudosymmetric as an alternative. Therefore, we conclude that our expectations for the eventual structure for these calumetite-like synthetic compounds are based on the oversimplified one-layer *P*4/*nmm* substructure, most probably in a frequent stacking pattern that would give a high probability to *C* centring, on average; i.e. the edge-sharing construction refined against synthetic data, above. This simplified two-layer substructure model in *Cmcm* may be further improved to account for all peaks evident, and the ¼ Ca per formula unit deficiency compared to centennialite, through site ordering over inequivalent Ca sites. This can force a reduction in symmetry, from one dominated by *Cmcm*, to a larger-lattice $P2_1/c$ model (with $\beta \approx 90°$). Such a construction indexes all observed peaks from synthetic calumetite-like material, Table 5.

Conclusions

The new mineral centennialite, from the Centennial Mine, Calumet, Houghton County Michigan, USA, is structurally characterized as a member of the atacamite group, similar to the kapellasites (trigonal, $P\bar{3}m1$, $Cu_3M^{2+}(OH)_6Cl_2$). It is the ordered, M^{2+} = Ca dominant member and distinguishes itself from the other kapellasites by the presence of variable interlayer water, promoting a CaO_8 unit that is found in other, larger, related structures such as murdochite. Expectations from ionic radius effects on eventual bond lengths should be promising for magnetic studies of frustrated spin systems. We estimate that Ca-containing kapellasites will provide the largest lattices available for this family. Centennialite occurs in visually heterogeneous assemblages of atacamite minerals and calumetite. We confirm that the synthetic $Cu_3(OH)_6CaCl_2{\cdot}H_2O$ phase produced by Erdös *et al.* (1981), JCPDS 35-1258, shares an identical lattice and an extremely similar chemistry and alongside the 'unidentified Cu-Ca-Cl mineral' of Heinrich and Robinson (2004) are almost certainly the same material as centennialite. We demonstrate a clear link between natural calumetite and centennialite in all the specimens studied; including Williams-donated and type material from the description of calumetite. Following the demonstration of Erdös *et al.* (1981), on a synthetic 'calumetite-like' $Cu_4CaCl_2(OH)_8{\cdot}3.5H_2O$ phase that on heating transformed to $Cu_3(OH)_6CaCl_2{\cdot}H_2O$, we illustrate that natural calumetite (from type material) also transforms on heating to a centennialite-like compound, strongly suggesting that the two synthetic and natural analogue phases are equivalent. Using data collected on our own synthetic calumetite material, we propose a substructure model for calumetite that is consistent with data collected from type specimens here and material proposed elsewhere as a synthetic analogue of calumetite.

Acknowledgements

The authors thank R.T. Downs and M. Candee of the Mineral Museum of the University of Arizona, and D. Nectoux and the late J-M. Le Cléac'h of the Musée de Minéralogie, Paris, for allowing access to their specimens of Williams' calumetite, as well as for agreeing to curate the centennialite samples. The ESRF is thanked for access to IHR beamtime at ID06. We also thank I. Snigireva (ESRF) for EDX investigation of the samples. This forms part of ongoing studies that has benefitted from access to beamline ID09A, through M. Hanfland and ID31, through A. Fitch and C. Drathen. Associated studies relevant to a larger array of synthetic compounds, which have no doubt influenced our thinking on centennialite, have also been conducted by C. Dela Cruz at HFIR of the Oak Ridge National Laboratory and of S. Margadonna of Swansea University. Our thanks are due also to A. Lubej (Cinkarna Celje) for offering access to samples of basic copper chlorides. We appreciate the contact with S. Carlson, who has

provided us with much local information, invaluable copies of Heinrich's *Mineralogy of Michigan* and the unpublished report of P. Brandes and G. Robinson. Revised manuscripts were improved using the comments of several anonymous Reviewers, the Structures Editor, P. Leverett, the Associate Editor, M. Rumsey and Principal Editor, P. Williams, who are all thanked for their considerable efforts.

References

Boultif, A. and Louër, D. (1991) Indexing of powder diffraction patterns for low-symmetry lattices by the successive dichotomy method. *Journal of Applied Crystallography*, **24**, 987–993.

Brandes, P.T. and Robinson, G.W. (2002) *A Preliminary Study of Calumetite and Other Copper Chloride Mineralization on the Keweenaw Peninsula, Michigan*. Unpublished MSc thesis, Michigan Technological University, USA.

Braithwaite, R.S.W., Mereiter, K., Paar, W.H. and Clark, A.M. (2004) Herbertsmithite, $Cu_3Zn(OH)_6Cl_2$, a new species, and a definition of paratacamite. *Mineralogical Magazine*, **68**, 527–539.

Christ, C.L. and Clark, J.R. (1955) The crystal structure of murdochite. *American Mineralogist*, **40**, 907–916.

Chu, S., McQueen, T.M., Chisnell, R., Freedman, D.E., Müller, P., Lee, Y.S. and Nocera, D.G. (2010) Cu^{2+} (S = ½) Kagomé antiferromagnet: $Mg_xCu_{4-x}(OH)_6Cl_2$. *Journal of the American Chemical Society*, **132**, 5570.

Clissold, M.E., Leverett, P. and Williams, P.A. (2007) The structure of gillardite, the Ni-analogue of herbertsmithite, from Widgiemooltha, Western Australia. *The Canadian Mineralogist*, **45**, 317–320.

Colman, R.H., Ritter, C. and Wills, A.S. (2008) Toward perfection: $Cu_3Zn(OH)_6Cl_2$, a new model S = ½ Kagome antiferromagnet. *Chemistry of Materials*, **20**, 6896–6899.

Colman, R.H., Sinclair, A. and Wills, A.S. (2011) Magnetic and crystallographic studies of Mg-herbertsmithite, γ-$Cu_3Mg(OH)_6Cl_2$ – A new S = ½ kagome magnet and candidate spin liquid. *Chemistry of Materials*, **23**, 1811–1817.

Dubler, E., Vedani, A. and Oswald, H.R. (1983) New structure determination of murdochite, Cu_6PbO_8. *Acta Crystallographica*, **C39**, 1143–1146.

Erdös, E., Denzler, E. and Altorfer, H. (1981) Thermochemical, crystallographic and infrared studies on calcium copper hydroxychloride hydrates. *Thermochimica Acta*, **44**, 345–361.

Fak, B. Kermarrec, E. Messio, L., Bernu, B., Lhuilier, C., Bert, F., Mendels, P., Koteswararo, B., Bouquet, F., Ollivier, J., Hillier, A.D., Amato, A., Colman, R. H. and Wills, A.S. (2012) *Physical Review Letters*, **109**, 037208.

Feitknecht, W. (1949) Über Doppelhydroxyde und basische Doppelsalze. 7. Über basische Doppelchloride des Kupfers. *Helvetica Chimica Acta*, **32**, 1653–1667.

Fleet, M.E. (1975) The crystal structure of paratacamite, $Cu_2(OH)_3Cl$. *Acta Crystallographica*, **B31**, 183–187.

Hammersley, A.P., Svensson, S.O., Thompson, A., Graafsma, H., Kvick, Å and Moy, J.P. (1995) Calibration and correction of distortions in 2D detector systems. *Review of Scientific Instruments*, **66**, 2729–2733.

Hammersley, A.P., Svensson, S.O., Hanfland, M., Fitch, A.N. and Häusermann, D. (1996) Two-dimensional detector software: from real detector to idealised image or two-theta scan. *High Pressure Research*, **14**, 235–248.

Heinrich, E.W. and Robinson, G.W. (2004) *Mineralogy of Michigan*. A. E. Seaman Mineral Museum, Michigan Technical University, Houghton, Michigan, USA.

Holland, T.J.B. and Redfern, S.A.T. (1997) Unit cell refinement from powder diffraction data: the use of regression diagnostics. *Mineralogical Magazine*, **61**, 65–77.

Jansen, O., Richter, J. and Rosner, H. (2008) Modified kagome physics in the natural spin-½ kagome systems: Kapellasite $Cu_3Zn(OH)_6Cl_2$ and haydeeite $Cu_3Mg(OH)_6Cl_2$. *Physical Review Letters*, **101**, 106403.

Jarek, U., Holynksa, M., Slepokura, K. and Lis, T. (2007) Calcium chloride rhenate(VII) dehydrate. *Acta Crystallographica,* **C63**, 77–79.

Kampf, A.R., Sciberras, M.J., Williams, P.A., Dini, M. and Donoso, A.A.M. (2013*a*) Leverettite from the Torrecillas miner, Iquique Province, Chile: the Co-analogue of herbertsmithite. *Mineralogical Magazine*, **77**, 3047–3054.

Kampf, A.R., Sciberras, M.J., Leverett, P., Williams, P.A., Malcherek, T., Schlüter, J., Welch, M.D., Dini, M. and Donoso, A.A.M. (2013*b*) Paratacamite-(Mg), $Cu_3(Mg,Cu)Cl_2(OH)_6$; a new substituted basic copper chloride mineral from Camerones, Chile. *Mineralogical Magazine*, **77**, 3133–3124.

Kermarrec, E., Zorko, A., Bert, F., Colman, R.H., Koteswararao, B., Bouquet, F., Bonville, P., Hillier, A., Amato, A., van Tol, J., Ozarowski, A., Wills, A.S. and Mendels, P. (2014) Spin dynamics and disorder effects in the S = ½ kagome Heisenberg spin-liquid phase of kapellasite. *Physical Review B*, **90**, 205103.

Krause, W., Bernhardt, H.J., Braithwaite, R.S.W., Kolitsch, U. and Pritchard, R. (2006) Kapellasite, $Cu_3Zn(OH)_6Cl_2$, a new mineral from Lavrion, Greece, and its crystal structure. *Mineralogical Magazine*, **70**, 329–340.

Krekel, C. and Polborn, K. (2003) Lime-blue – A mediaeval pigment for wall paintings? *Studies in Conservation*, **48**, 171–182.

Kumar, G.N.H., Parthasarathy, G. and Rao, J.L. (2011) Low-temperature electron paramagnetic resonance

studies on natural calumetite from Khetri copper mine, Rajasthan, India. *American Mineralogist*, **96**, 654–658.

Le Bail, A., Duroy, H. and Fourquet, J.L. (1988) Ab initio structure determination of $LiSbWO_6$ by X-ray powder diffraction. *Materials Research Bulletin*, **23**, 447–452.

Leoni, M., Gualtieri, A.F. and Roveri, N. (2004) Simultaneous refinement and microstructure of layered materials. *Journal of Applied Crystallography*, **37**, 166–173.

Li, Y. and Zhang, Q.M. (2013) Structure and magnetism of S = ½ kagome antiferromagnets $NiCu_3(OH)_6Cl_2$ and $CoCu_3(OH)_6Cl_2$. *Journal of Physics: Condensed Matter*, **25**, 026003.

Li, Y., Fu, J.L., Wub, Z.H. and Zhang, Q.M. (2013) Transition-metal distribution in kagome antiferromagnet $CoCu_3(OH)_6Cl_2$ revealed by resonant X-ray diffraction. *Chemical Physics Letters*, **570**, 37–41.

Lubej, A., Koloini, T. and Pohar, C. (2004) Industrial precipitation of cupric hydroxyl-salts. *Acta Chimica Slovenica*, **51**, 751–768.

McQueen, T.M., Han, T.H., Freedman, D.E., Stephens, P. W., Lee, Y.S. and Nocera, D.G. (2011) $CdCu_3(OH)_6Cl_2$: a new layered hydroxide chloride. *Journal of Solid State Chemistry*, **184**, 3319–3323.

Malcherek, T. and Schlüter, J. (2007) $Cu_3MgCl_2(OH)_6$ and the bond-valence parameters of the OH-Cl bond. *Acta Crystallographica*, **B63**, 157–160.

Malcherek, T., Bindi, L., Dini, M., Ghiara, M.R., Donoso, A.M., Nestola, F., Rossi, M. and Schlüter, J. (2014) Tondiite, $Cu_3Mg(OH)_6Cl_2$, the Mg-analogue of herbertsmithite. *Mineralogical Magazine*, **78**, 583–590.

Nilsen, G.J., de Vries, M.A., Stewart, J.R., Harrison, A. and Ronnow, H.M. (2013) Low-energy spin dynamics of the S = ½ kagome system herbertsmithite. *Journal of Physics: Condensed Matter*, **25**, 106001.

Nishio-Hamane, D., Momma, K., Ohnishi, M., Shimobayashi, N., Miyawaki, R., Tomita, N. and Minakawa, T. (2014) Misakiite, IMA 2013-131. CNMNC Newsletter no. 20, June 2014, page 552. *Mineralogical Magazine*, **78**, 549–558.

Oswald, H.R. and Feitknecht, W. (1964) Über Hydroxyhalogenide $Me_2(OH)_3Cl$, -Br, -J zweiwertiger Metalle (Me = Mg, Ni, Co, Cu, Fe, Mn). *Helvetica Chimica Acta*, **47**, 272–289.

Petříček, V., Dušek, M. and Plantinus, L. (2014) Crystallographic Computing System JANA2006: General features. *Zeitschrift für Kristallographie*, **229**, 345–352.

Schlüter, J. and Malcherek, T. (2007) Haydeeite, $Cu_3MgCl_2(OH)_6$, a new mineral from the Haydee mine, Salar Grande, Atacama desert, Chile. *Neues Jahrbuch für Mineralogie*, **184**, 39–42.

Syozi, I. (1951) Statistics of the kagome lattice. *Progress of Theoretical Physics*, **6**, 306–308.

Taupin, D. (1973) A powder-diagram automatic-indexing routine. *Journal of Applied Crystallography*, **6**, 380–385.

Wannier, G.H. (1950) Antiferromagnetism – the triangular net. *Physical Review*, **79**, 237–364.

Welch, M.D., Sciberras, M.J., Williams, P.A., Leverett, P., Schlüter, J. and Malcherek, T. (2014) A temperature-induced reversible transformation between paratacamite and herbertsmithite. *Physics and Chemistry of Minerals*, **41**, 33–48.

Williams, S.A. (1963) Anthonyite and calumetite, two new minerals from Michigan copper district. *American Mineralogist*, **48**, 614–619.